



Influence of Vanadium Oxide on the Optical and Electrical Properties of Li (Oxide or Fluoride) Borate Glasses

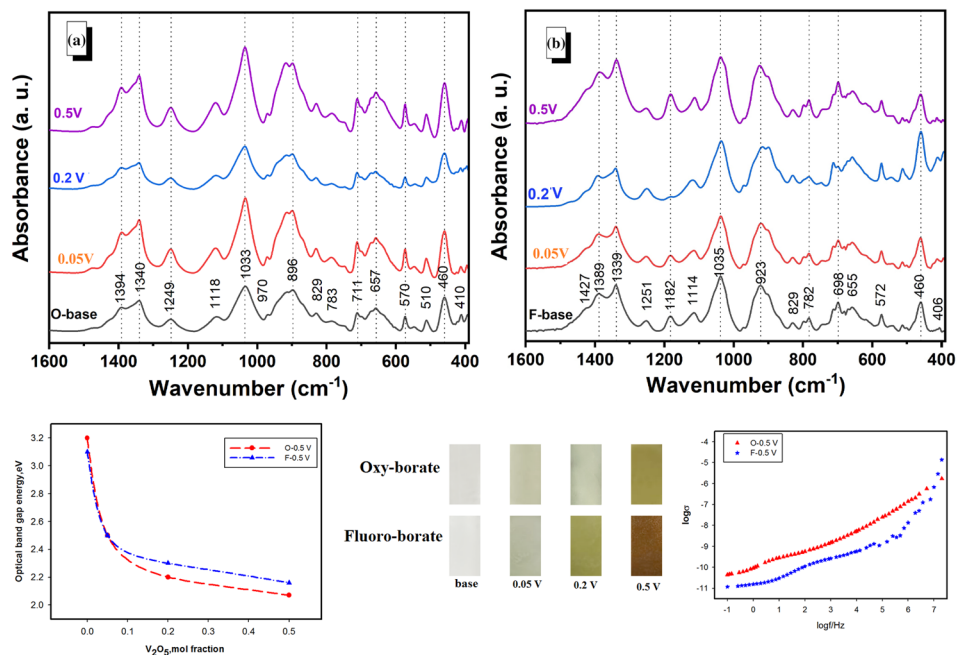
Amal M. Abdel-karim¹ · A. M. Fayad² · I. M. El-kashef³ · Hisham A. Saleh⁴

Received: 19 September 2022 / Accepted: 19 December 2022 / Published online: 13 January 2023
© The Author(s) 2023

Abstract

Binary glass systems of the chemical composition $0.25\text{Li}_2\text{O}-0.75\text{B}_2\text{O}_3$ and $0.25\text{LiF}-0.75\text{B}_2\text{O}_3$ with different additive ratios of V_2O_5 were prepared using the melt-quenching method. Characterization was carried out through different techniques such as Fourier-transform infrared (FTIR) and ultraviolet–visible absorption (UV–visible) spectroscopy. Optical and electrical properties have been investigated in order to recognize the role of V_2O_5 in glass. FTIR spectra of the studied glasses expose repetitive vibration curves with limited variations. BO_4 and BO_3 are the basic constituent units of the studied glasses in addition to the BO_2F and BO_3F units in the case of fluoro-borate glasses. Shifting to a higher wavelength in the optical absorption spectra and a decrease in the optical band gap values via increasing V_2O_5 content confirms the formation of non-bridging oxygen (NBO). The ac-electrical conductivity (σ_{ac}) and the dielectric constants (ϵ') of the glass samples were studied in the frequency range 10^2 Hz–8 MHz. The ionic conduction takes place by Li-ion movement in all samples. The electronic conduction of borate glass can be explained using hopping between V^{4+} and V^{5+} . The results show excellent properties of the glass with a low concentration of vanadium oxide.

Graphical Abstract



Keywords Borate glass · LiF · Li_2O · V_2O_5 · energy band gap · optical and electrical properties

Extended author information available on the last page of the article

Introduction

Glass plays a vital role worldwide, especially in science and industry. The amorphous structure of glasses is a unique physical state that differs greatly from crystals and other material forms. Transition metal oxides (TMO) have excellent optical and electronic properties and can be utilized in various scientific and industrial fields. Modified oxide glasses that contain transition metal ions are of great interest as semiconducting materials. They have potential applications such as optoelectronic devices, solid-state batteries, memory switching, and cathode materials.^{1,2} These glasses are known as mixed ionic-electronic conductors, the ionic conduction depending on the alkali ion concentration. At the same time, the electronic conductivity is owing to the unpaired electron hopping between high- and low-valence states within the polyvalent transition ions.

Glassy structures of different compositions can be synthesized using glass formers and additive materials.³ The characteristic feature of borate glasses is a glass network that mainly consists of BO_4 and BO_3 units. The presence and conversion between these groups are fundamentally dependent on the glass modifier content as alkali and alkaline earth oxides. The presence of the different fractions of the coordinated boron units provides the possibility of fine physical properties.

The addition of alkali oxides such as lithium oxide (Li_2O) to the glassy borate network, modifies the glass structure.⁴ Non-bridging oxygen (NBO) will be achieved if the Li_2O content exceeds 25%.⁵ At Li_2O less than 25%, the triangle units BO_3 sp^2 are changed to tetra-borate units BO_4 sp^3 . BO_4 unit is connected to two other BO_4 units and the structure leads to the formation of long chains. Lithium borate glasses are of great technological interest due to their multiple uses in a large range of electrochemical applications, solar energy converters, and high-density energy batteries. Lithium ions within the glass network act as ionic conductors. In the presence of fluoride ions in borate glass, some BO_2F and BO_3F are formed. These modifications affect the properties of borate glass.⁶

Vanadium-doped glasses show a semiconducting nature. Vanadium is a strong transition metal that is preferred for use in different applications such as solar cells, optoelectronics, and radiation shielding due to its unpaired electron and the different oxidation states (V^{3+} , V^{4+} , and V^{5+})^{7,8} in glass matrix according to the quantity of the modifiers, the structure of the host-glasses, the ions size, and their field strength.^{9–12} The presence of V_2O_5 in these glasses is used as a colorant for semiconductors applied in memory-switching applications,^{13–15} and gamma radiation shielding,^{10,14,15} where the properties of oxide glasses

are mainly related to the state of the vanadium ions, the number of vacancies (defects), and the glass structure.^{11,16} Various spectral and electrical studies of different glasses doped with relatively high ratios of vanadium have been carried out as phosphate^{2,17–19} borosilicate,¹ Sr-borate,¹⁶ Bi-borate^{5,6} and mixed alkali fluoro-borate.¹⁴ However, studies on glasses doped with low ratios of vanadium oxide are limited.

Vanadium ions are expected to dissolve easily in the borate network because some of the infrared vibrational bands of these ions lie in the same region as those of the BO_4 and BO_3 units.²⁰

The present work is concerned with structural studies on two binary glass systems, lithium (oxy and fluoro) borate glass doped with low mol.% (0.05, 0.2, and 0.5) of V_2O_5 . The purpose is to check the effect of the various factors on ac-electrical conductivity, permittivity, and electrical modulus. The Li-borate glass containing LiF instead of Li_2O was prepared to study the effect of the presence of fluoride ions on the electrical properties and the effect of different low concentrations of vanadium oxide on both prepared Li-borate glasses. FTIR, optical properties, band gap calculations, and electrical measurements were carried out, achieving the predicted results and confirming the stable vanadium valence states in these glass systems.

Experimental

Materials and Methods

Binary glass systems of (oxy and fluoro) lithium borate of chemical composition $(0.25\text{Li}_2\text{O}-0.75\text{B}_2\text{O}_3)$ and $(0.25\text{LiF}-0.75\text{B}_2\text{O}_3):x\text{V}_2\text{O}_5$, where x is varied at 0.05 mol.%, 0.2 mol.%, and 0.5 mol.%, were prepared using the melt-quenching method. The glass samples with chemical composition were encoded and are listed in Table I. High-purity chemical materials of orthoboric acid (H_3BO_3 , 99% from Nasr Lab, Egypt), lithium carbonate (Li_2CO_3 , 99.9%, Sigma Aldrich), and lithium fluoride were used as the starting materials for

Table I The chemical composition of the glass samples

| Glass samples | | B_2O_3 | Li_2O | LiF | V_2O_5 |
|---------------|----------|------------------------|-----------------------|------|------------------------|
| Oxy-borate | O-base | 0.75 | 0.25 | – | – |
| | O-0.05 V | 0.75 | 0.25 | – | 0.05 |
| | O-0.25 V | 0.75 | 0.25 | – | 0.20 |
| | O-0.5 V | 0.75 | 0.25 | – | 0.50 |
| Fluoro-borate | F-base | 0.75 | – | 0.25 | – |
| | F-0.05 V | 0.75 | – | 0.25 | 0.05 |
| | F-0.25 V | 0.75 | – | 0.25 | 0.20 |
| | F-0.5 V | 0.75 | – | 0.25 | 0.50 |

B_2O_3 , Li_2O , and LiF , respectively. Vanadium oxide (V_2O_5 99.6%, Sigma Aldrich) was used as a dopant. The weighted fractions of their powder were mixed well before melting in a silica crucible for 30 min at $450^\circ C$, then the temperature was raised to $1150^\circ C$ for 1 h in an electrical furnace with occasional rotating of the crucible, to eliminate the bubbles and ensure that all components were completely homogenized. Then melted glass samples were poured into stainless steel molds of selected dimensions, then immediately transferred to annealing preheated furnace regulated at $300^\circ C$ and cooled gradually at a rate of $30^\circ C/h$. The glass samples were of faint green color that changed with increasing vanadium oxide content, but the base sample was colorless, as displayed in Fig. 1.

Characterization Techniques

X-Ray Diffraction (XRD)

XRD spectra of the glass samples were determined using a Bruker diffractometer (Bruker D8 Advance) with a target $Cu\ K\alpha$ radiation source ($\lambda = 1.5405\ \text{\AA}$) and a scanning rate $0.2\ \text{min}^{-1}$.

FTIR and UV Analysis

Fourier transform infrared (FTIR) studies were performed on the ground powder of the glass samples through the KBr method in the range $400\text{--}4000\ \text{cm}^{-1}$ using a computerized Fourier transform infrared spectrometer (FT/IR-4600, JASCO Corp., Japan).

Ultraviolet–visible absorption (UV–visible) and transmission spectra were acquired for the polished glass samples of thickness $3\ \text{mm} \pm 0.1\ \text{mm}$ using a double-beam spectrophotometer (JASCO V-570, Japan) over the range of $200\text{--}2500\ \text{nm}$ with accuracy of ± 0.002 absorbance and $\pm 0.3\%$ transmittance.

The optical band gap energies E_g of the prepared glasses were estimated from the Tauc equation.^{12,21} Absorption coefficient α was calculated from the Beer–Lambert relation:

$$\alpha(n) = \frac{2.303A}{t} \quad (1)$$

where A is absorbance and t is the thickness. Tauc plots were obtained from the relation

$$(\alpha hv)^n = A(hv - E_g) \quad (2)$$

where A is the proportionality constant depends on the nature of the material, h is Planck's constant, ν is the frequency, and n is the indirect transition. In the Tauc equation, the plot of $(\alpha hv)^n$ versus photon energy (hv) for the investigated sample leads to the design of a certain curve, and the intersection of the extrapolated linear portion of this curve with the (hv) axis is used to obtain E_g .

Electrical Studies

The electrical properties of the polished glass samples were investigated in frequencies ranging from $10^2\ \text{Hz}$ to $8\ \text{MHz}$ using an RLC Bridge (HIOKI model 3532, Japan). The prepared samples as a disc were placed between the two electrodes.

It is well known that the ac-electrical conductivity, σ_{ac} , is frequency-dependent and consists of two terms according to

$$\sigma_{ac}(\omega) = \sigma_{tot}(\omega) - \sigma_{dc}(T) \quad (3)$$

where $\sigma_{dc}(T)$ is dc-electrical conductivity and $\sigma_{tot}(\omega)$ is total electrical conductivity. The term $\sigma_{ac}(\omega)$ can be written in the form of a power law as²²

$$\sigma_{ac}(\omega) = A(\omega)^s \quad (4)$$

where $\omega = 2\pi f$ is the angular frequency and s is the composition-dependent parameter obtained from the slope of these lines.²³

The dielectrics are an important property of semiconductor material. In this study, the real part of the dielectric constant ϵ' was calculated from the measured capacitance at all frequencies under consideration according to the following equations²⁴

$$\epsilon' = C \cdot \frac{t}{A\epsilon_0} \quad (5)$$

where ϵ_0 is the permittivity of the free space.

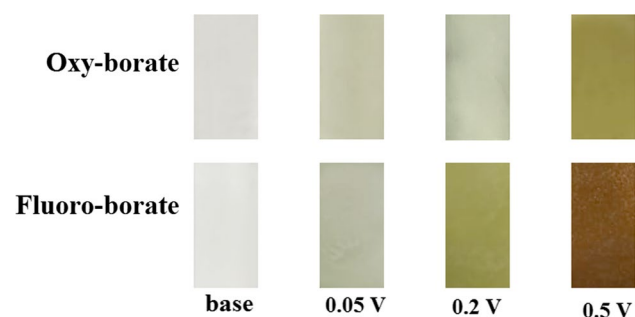


Fig. 1 Photographs of the prepared glass samples.

Results and Discussion

X-Ray Diffraction (XRD)

Figure 2 shows XRD patterns of 0.5 mol.% vanadium (Li_2O or LiF) borate glasses. The absence of sharp peaks over a

wide range of diffraction angles confirms the amorphous nature of the glass samples.

FTIR Absorption Spectra of the Two Binary Glass Systems

The infrared absorption spectra of the two binary glass systems were recorded to obtain detailed information on the arrangements of the different structural units in the glass network. Figure 3a, b demonstrate the IR spectra of the LiO–B₂O₃ and LiF–B₂O₃ glasses with and without V₂O₅ doping. The IR spectra of the two base glasses reveal a close analogy of several bands and peaks related mainly to the borate groups that constitute the glass network.

It is accepted by several studies on fluoro-borate glasses that due to the analogous masses and almost equal radii of

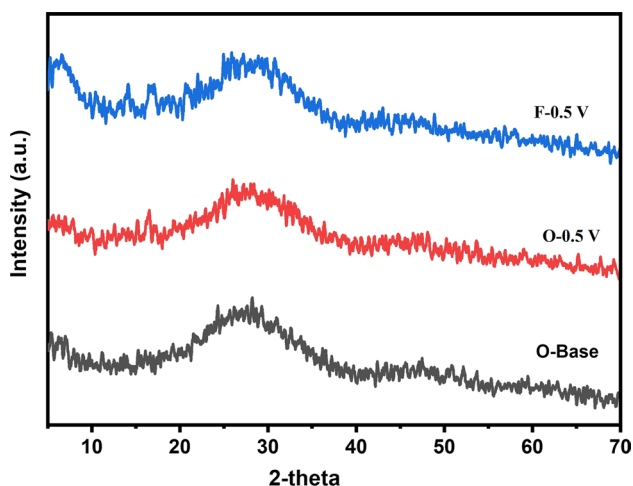


Fig. 2 XRD pattern of the prepared glass.

oxygen and fluorine, major variations are not expected to be identified in the mid-IR spectra.^{25,26} The fluoride ions in the borate glass network cause some structural modifications where some BO₃ and BO₄ species are modified to be BO₂F and BO₃F structural units, and the absorption in the regions 1200–1600 and 800–1200 cm⁻¹ can be associated with their oscillations, respectively.^{25,27,28} Therefore, the current IR absorption peaks of the undoped glasses (base) can be attributed to their B–O vibration modes as follows:

1. The absorption peaks at 410 cm⁻¹, 460 cm⁻¹, 510 cm⁻¹, and 545 cm⁻¹ within the wavenumber range 400–550 cm⁻¹ can be correlated to vibrations of cation ions (Li⁺, Na⁺, Ca²⁺), as well as the distinct band at 460 cm⁻¹, which is related to the alteration of B–O–B bond angle, while the bands 570 cm⁻¹ is assigned to O–B–O winding oscillations as suggested by several authors.^{29–32}
2. The bands located at 600–800 cm⁻¹ are due to O₄B–O–BO₃ twisting oscillations caused by bending oscillation modes of different borate units.^{13,14,33}
3. The mid-IR range 800–1200 cm⁻¹ contains the characteristic vibration modes of the B–O bond of the (BO₃–O) units that are represented in the spectra by wave numbers at 896 cm⁻¹, 914 cm⁻¹, 970 cm⁻¹, 1033 cm⁻¹, and 1118 cm⁻¹.²⁵
4. The absorption peaks positioned at 1249 cm⁻¹, 1340 cm⁻¹, 1394 cm⁻¹, and 1431 cm⁻¹ extending into the IR region 1200–1600 cm⁻¹ represent the oscillation modes of B–O linkages in BO₃ or (BO₂O)⁻ species.³²

On doping the V₂O₅ in increasing amounts (0.05 mol.%, 0.2 mol.%, 0.5 mol.%), the IR spectra were retained in nearly the same number and position of IR absorption vibration bands. It should be mentioned that the recognized bands

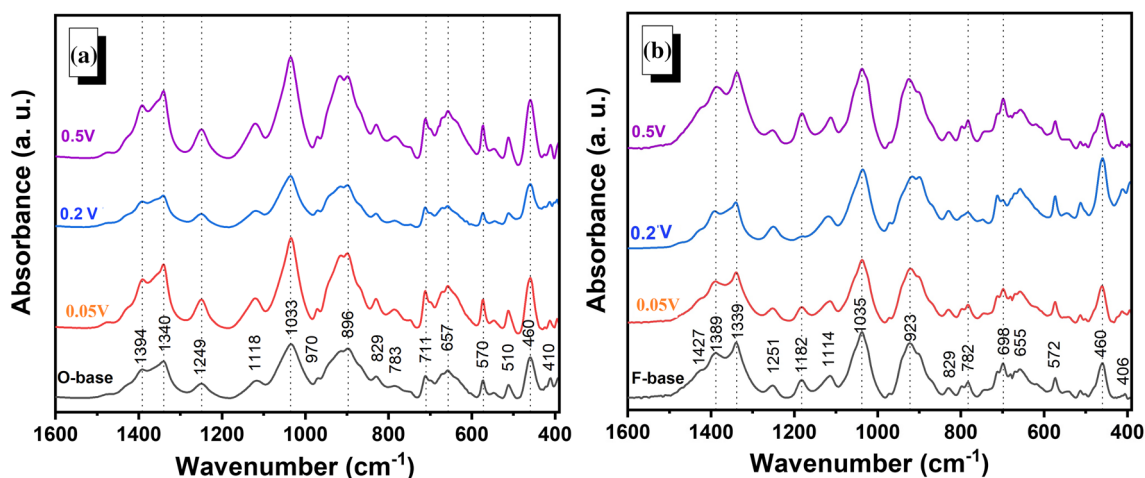


Fig. 3 FTIR absorption spectra (a) oxy- and (b) fluoro-lithium borate glasses with and without V₂O₅ doping

at $800\text{--}1200\text{ cm}^{-1}$ and $1200\text{--}1600\text{ cm}^{-1}$ became clearer than that in the spectra of base glass. The intensity of peaks centered at 880 , 1035 , and 1348 cm^{-1} with respect to the V–O–V links and the vibration of the V=O group in the

VO_2 polyhedra and the formation of B–O–V units increased, respectively.^{11,13,15} Thus, this indicated that the vanadium ions in glass lattice create non-bridging oxygen linkages (NBOs) or B–O–V chains which could be found in the V^{4+} state with vanadyl complexes.

Optical Studies

Ultraviolet and visible transmittance spectra were obtained for finely polished glasses of Li-borate glasses without and with different amounts of V_2O_5 are given in Fig. 4. It is clear from these spectra that the UV–Visible transmittance of the oxy and fluoro Li-borate glasses decreases with the addition of $0.05\text{ mol.}\%$ V_2O_5 , indicating that the V ions change the band structure of the glasses, reducing the optical transition, and then increase again with increasing V_2O_5 . The transparency of 0.5 V gradually increases from $\sim 600\text{ nm}$ to 2500 nm .

Figure 5 shows the absorption spectra of the two binary glass systems ($\text{Li}_2\text{O–B}_2\text{O}_3$) and ($\text{LiF–B}_2\text{O}_3$) as a base and V_2O_5 -doped glasses ($0.05\text{ mol.}\%$, $0.2\text{ mol.}\%$, and $0.5\text{ mol.}\%$). The UV absorption spectra of vanadium-free glasses show strong peaks that are attributed to trace iron impurities of the used raw materials.^{10,13,34} Even small concentrations of vanadium ions cause an electron transfer, including the transition of an electron from the coordinating orbital of an oxygen atom to an orbital of the metal ion. The spectra absorption is very close to undoped glasses in addition to other peaks with high-intensity shifts to longer wavelength (redshift) with increasing vanadium concentration as listed in Table II. This suggests that the non-bridging oxygen is increasing with the increase in vanadium.

The possible valance states of vanadium ions in glasses are V^{+5} , V^{4+} , and V^{3+} as confirmed through extended optical studies.^{10,13,15} The UV absorption is observed to extend to a peak at 350 nm in oxy-borate, while there are two

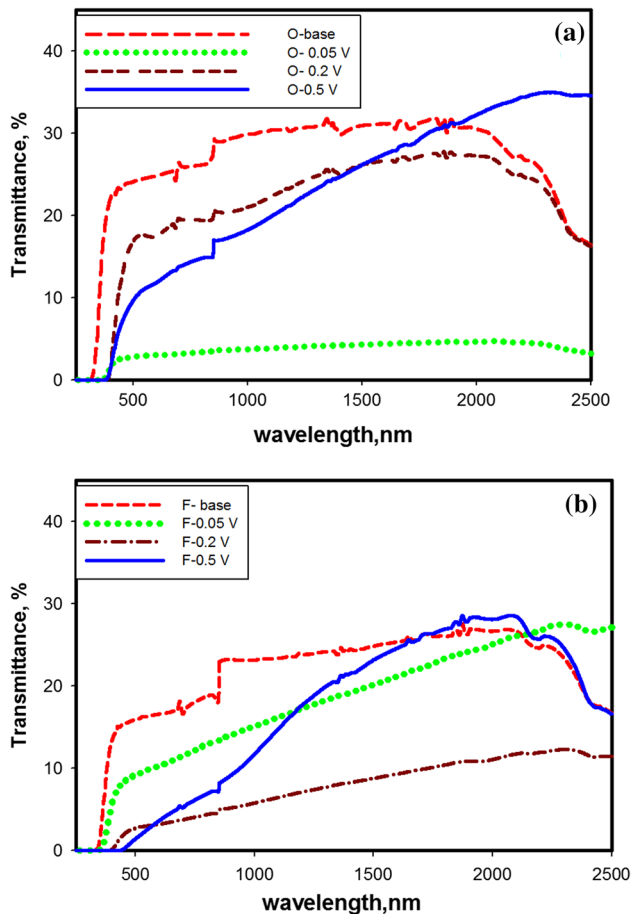


Fig. 4 Optical transmittance spectra of (a) Li_2O and (b) LiF borate glasses undoped and doped with different mol.% of Vanadium oxide.

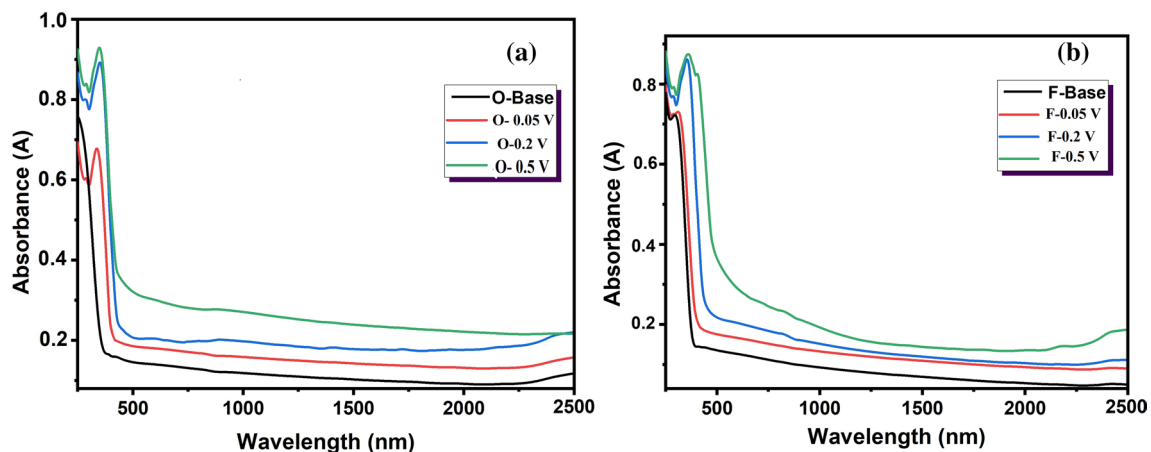


Fig. 5 The UV–Vis absorption spectra (a) oxy-borate and (b) fluoro-borate undoped and V_2O_5 -doped glasses.

peaks at 350 and 410 nm in the fluoro-borate glasses. It is accepted that V^{5+} ions provide a charge transfer absorption band around 380 nm where it belongs to the $3d^0$ configuration and has no free electrons to exhibit visible absorption.^{2,15} This means that the energy gaps are impacted by the proportion of vanadium ions and their possibility to form non-bridging oxygen (NBO) within the network. The similar performance of the non appearance of the visible peaks was detected when lower fractions of transition metal oxide as cupric oxide (0.04% and 0.1% CuO) doped lithium phosphate glass² and (0.5–2 mol.% vanadium oxide) doped mixed alkali borate glass.¹³

The band gap of the prepared binary glass was determined by Tauc's equation as mentioned in the experimental section. Figure 6 represents the Tauc plot $(\alpha h\nu)^{1/2}$ versus $(h\nu)$ and E_g . The band gap energy was determined

Table II The cut off wavelength, the optical band gap values of glass samples

| Sample | V ₂ O ₅ (mol %) | Cut-off wavelength, nm | E_g , eV (from cut-off wavelength) | E_g , eV (from Tauc relation) |
|----------|---------------------------------------|------------------------|--------------------------------------|---------------------------------|
| O-base | 0 | 358 | 3.46 | 3.2 |
| O-0.05 V | 0.05 | 406 | 3.05 | 2.5 |
| O-0.2 V | 0.2 | 425 | 2.91 | 2.2 |
| O-0.5 V | 0.5 | 438 | 2.8 | 2.07 |
| F-base | 0 | 368 | 3.36 | 3.1 |
| F-0.05 V | 0.05 | 412 | 3.01 | 2.5 |
| F-0.2 V | 0.2 | 432 | 2.87 | 2.3 |
| F-0.5 V | 0.5 | 512 | 2.42 | 2.16 |

by extrapolating the linear portion of the curve intersecting the $h\nu$ axis at $(\alpha h\nu)^{1/2} = 0$. Optical transition glasses are associated with absorbing phonons such as electronic behavior between the conduction and valence bands.³⁵ The energy band gap is also calculated from the cut-off wavelength. The calculated E_g listed in Table II lies in the same range as reported for semiconductors.³⁶ The E_g value decreases with increasing doped V₂O₅ for all the glasses. This means that there are several changes in the network structure due to intercalation of the doped V₂O₅ in the glass samples. The vanadium ions proceed as the defect centers close to the Fermi level. The transition occurs from the valence band to the vanadium sites and finally from the site of the defect to the conduction band. This performance may be attributed to the structural modifications that lead to increasing the NBO due to the presence of vanadium ions in the glass matrix.³⁷

The values of the optical band gap vary between 2.1 eV and 3.2 eV¹³ as listed in Table II. Figure 7 displays the relationship between the optical band gap and the vanadium content. The values decreased with the increase in vanadium content from 3.2 eV to 2.07 eV and from 3.1 eV to 2.16 eV for oxy and fluoro Li borate glasses, respectively, which is related to the intercalation of vanadium ions in the glass matrix that form NBO bonds and introduce a new level of impurities between the conduction and valence bands, as reported previously.^{38,39} On increasing V₂O₅ content, the E_g decreases due to the structural changes by conversion of BO₃ to BO₄ with increasing NBOs.

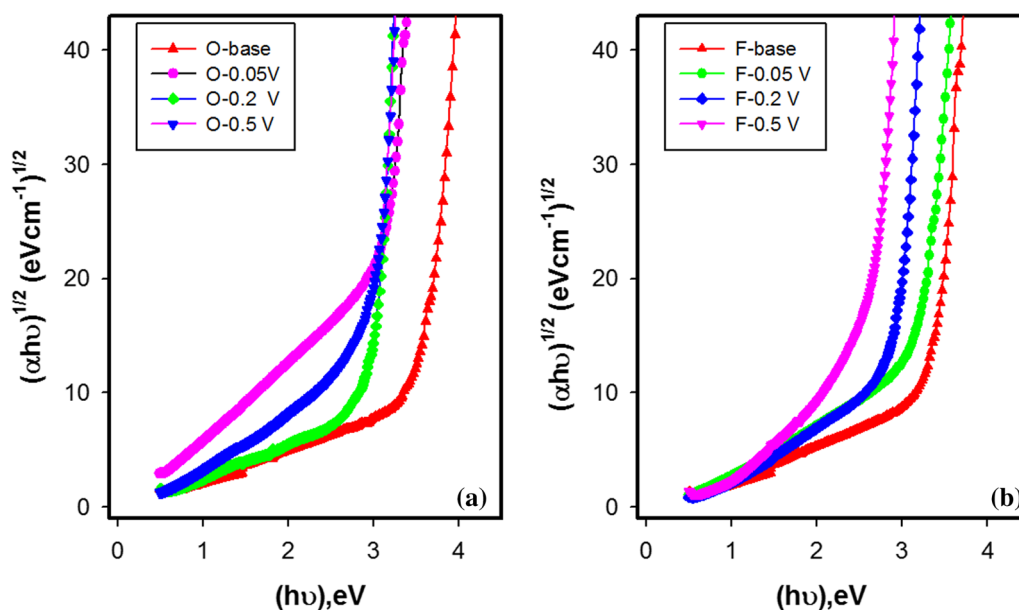


Fig. 6 Tauc plots for (a) Li₂O and (b) LiF glasses undoped and doped with different concentrations of vanadium oxide.

Electrical Properties

The electrical properties of the prepared glass samples were investigated by keeping the molar ratio of the network (B_2O_3) constant while increasing the V_2O_5 in the presence of an ionically active network (Li_2O or LiF).

The electrical properties including ac electrical conductivity, dielectric constant, and electrical modulus of the prepared Li_2O or LiF glasses undoped and doped with V_2O_5 were studied at room temperature and a frequency range from 10^2 Hz to 8 MHz.

Figure 8 shows the frequency dependence of the ac-electrical conductivity for the undoped and vanadium oxide-doped glasses. The conductivity increases with frequency, indicating that the glass samples have a semiconducting

nature. It can be concluded that samples doped with vanadium can be used as energy storage material in electronic devices. This relation is characterized by a plateau region at low frequencies matching the dc-conductivity¹⁷ and the dispersion region at high frequencies (frequency-dependent conductivity), showing that the conductivity increases with frequency implying conductivity relaxation.^{17,40} Borate glass with a structure composed of B_2O_3 is an insulator and insensitive to ionic migration because it requires high energy to produce B^{3+} ions. In the base Li_2O glass samples free of vanadium, the conduction process is mainly due to the contribution of Li^+ ions.⁴¹ The ionic conduction takes place by the mobility of Li ions in all samples. This structural change may convert BO_3 units into BO_4 structural units by creating more bridging oxygen networks and enhancing the compactness of the glass system leading to a conductivity decrease. It is found that the beginning of LiF instead of Li_2O decrease ionic conductivity due to the formation of local coulombic traps of fluorine ions, which delay the motion of Li ions.¹⁸ Doping transition metal ions in lithium borate glasses enhances their electrical properties due to hopping of a mobile electron from a low- to a high-valance state. Therefore, the addition of V ions creates paths for the movement of the charge carriers (Li ions) increasing the ac-conductivity. As a result, the electrical parameters were changed, which involved two different mechanisms.⁴² One is associated with ionic conduction due to the motion of lithium ions. On the other hand, with increased vanadium content, the electronic conduction increased due conversion of V^{4+} into V^{5+} ions.⁴³ The conductivity results support the IR spectra and indicate the presence of V^{5+} . The conduction path could be recognized by the NBO allowing the

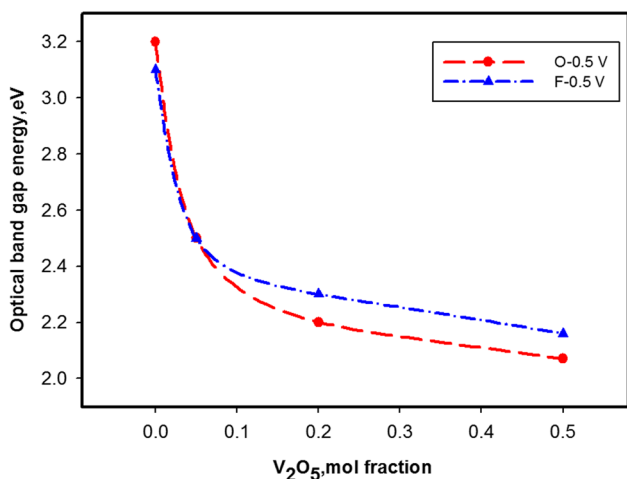


Fig. 7 The dependence of E_g on V_2O_5 content.

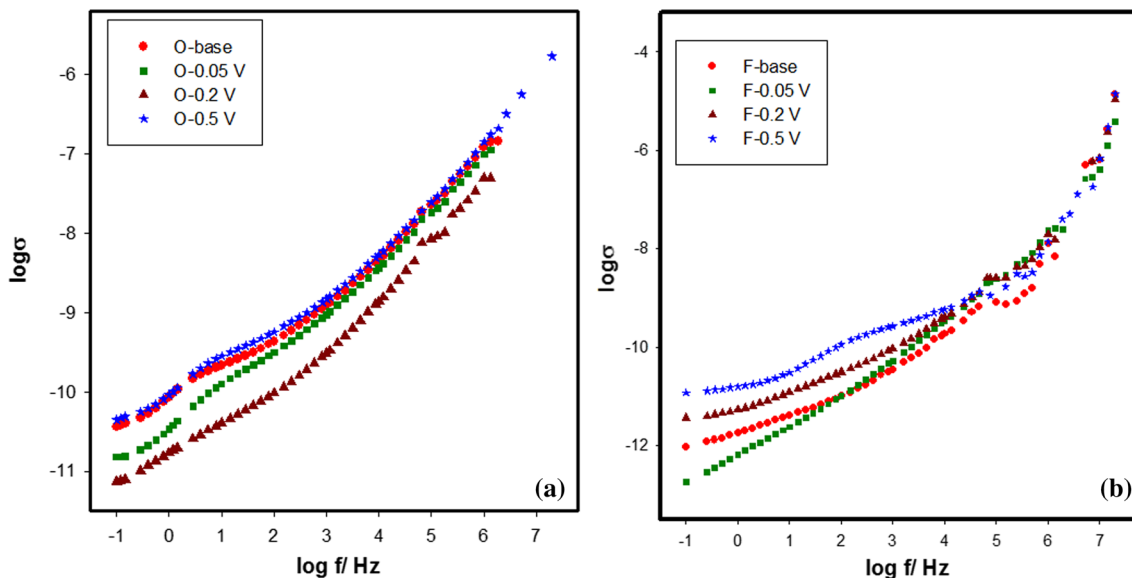


Fig. 8 Ac-electrical conductivity of (a) Li_2O and (b) LiF borate glasses doped with vanadium oxide.

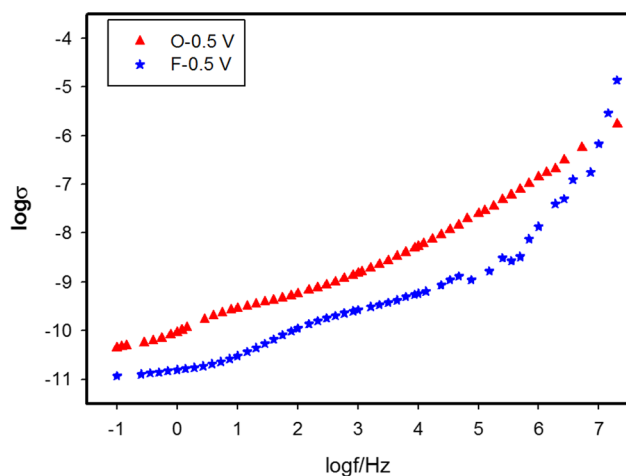


Fig. 9 The ac-conductivity of Li_2O and LiF doped with 0.5 mol.% V_2O_5 .

disruption of Li ions through the glass matrix and another way is the electronic transfer.

The conductivity increases slightly with increasing vanadium content in Li_2O at low and high frequency. But in LiF , with increasing vanadium content the conductivity increases at a low frequency and increases slightly at a high frequency. As shown in Fig. 9, the conductivity of Li_2O borate glass is higher than LiF borate glass doped with 0.5 mol.% V_2O_5 . This increase is related to the increase in the mobility of lithium ions and the electron transfer from the lower to higher valence state. The presence of non-bridging oxygen leads to expansion in the glass structure and facilitates the Li ion mobility, and subsequently the ionic conductivity increases.^{44,45} The slight increase in conductivity can be taken as a basis to rule out the role of F^- ions as the charge carriers in $\text{LiF-B}_2\text{O}_3$ glasses. Therefore, the electronic conduction in these glasses is mainly due to the transport of Li ions rather than F^- ions.

Figure 8 shows that the ac-electrical conductivity increases with two different rates; it increases at a slow rate in the low-frequency region, followed by a remarkable increase at high frequency, i.e., it follows a power law relation $A\omega^s$ ¹⁷ The behavior of ac-electrical conductivity obeys a power law relation²² which gives the relevant hopping mechanism.²⁴ The exponent 's' calculated from the slope of Fig. 8 using Eq. 11 measures the degree of interaction with the surrounding and also depends on the glass composition. Figure 10 shows the variation of calculated s values with mol.% of V_2O_5 . Exponent s decreases with increasing V content due to the formation of NBO atoms disrupted in the glasses.⁴⁰ The reduced exponent seen for mixed glasses

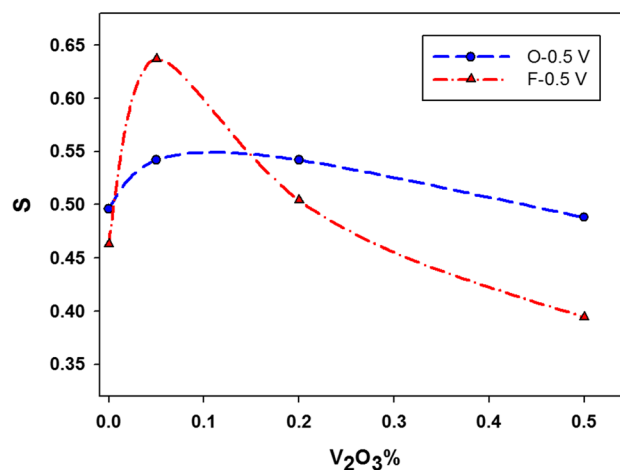


Fig. 10 Variation of s with V_2O_5 content.

could be coupled with a reduction of the pathways over that in the single oxide glasses.

Figure 11 shows the frequency dependence of the real part of dielectric constant ϵ' for Li_2O and LiF borate glass with and without different concentrations of vanadium oxide. For all glasses, ϵ' decreases with frequency. The decreasing numbers of dipoles cause a decrease in dielectric constant. At low frequency, ϵ' is high and falls with increasing frequency and then becomes constant above 10^4 Hz. The increase of V_2O_5 forms NBO and prolongs the structure of the glass network, which increases the dielectric values.

The high value of the dielectric constant at a low frequency decreases rapidly with increasing frequency. The high value is due to the presence of an electric field which helps the electrons jump between filled and unfilled sites.⁴⁶ At high frequency, minor decreases are observed because the dipoles cannot rotate, so the oscillation starts to lie behind the field. It has been shown that the dielectric constant at 10^2 Hz is found to be 37.04, 32.43, 19.57, and 43.51274, 95, 121, 117 for base glass and 0.05 mol.%, 0.025 mol.%, and 0.5 mol.% V_2O_5 , respectively, for Li-O borate glasses. However, for Li-F borate glasses the dielectric constants are 9.29, 7.98, 11.65, and 17.05. It is seen that the values of ϵ' increased with the addition of vanadium oxide.

The dielectric constant is affected by polarizations (electronic, ionic, dipolar, and space charge). The space charge depends on the purity of the glasses. Its action is noticeable in the low-frequency region. The vanadium ions present as modifiers weaken the network and construct pathways,⁴⁷ and higher ϵ' due to the lithium ions hop easily^{48,49} Under the

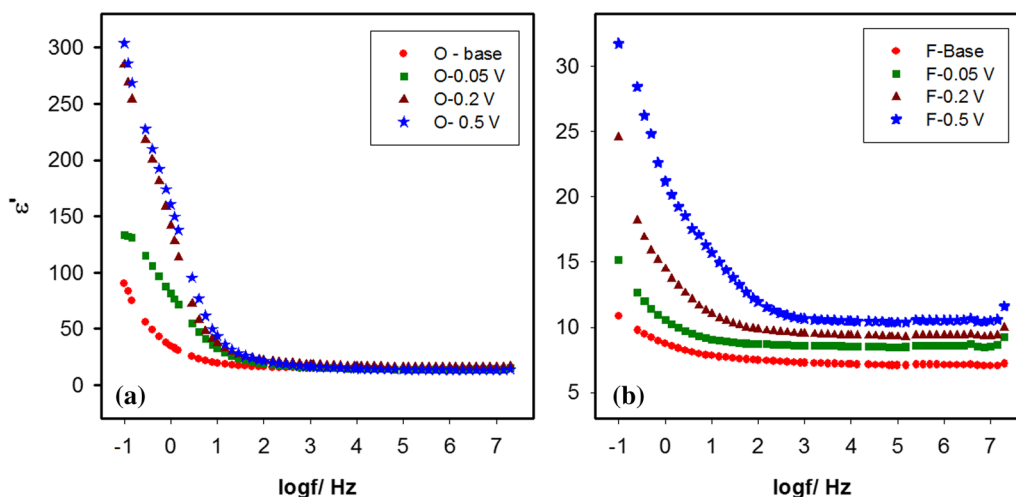


Fig. 11 The variation of permittivity with frequency of undoped and doped (a) Li₂O and (b) LiF borate glasses with vanadium oxide.

electric field, lithium ions move through the network. However, at high frequencies, mobility is impeded.

The electrical modulus of conducting materials was used to study electrical relaxation.⁵⁰ The benefit of this illustration is the effects of electrode polarization are minimized. The *M'* and *M''* real and imaginary parts of the electric modulus as a function of frequency are shown in Figs. 12 and 13. Figure 12 shows that the electric modulus *M'* goes to zero at low frequencies signifying a slight polarization,¹⁹ while *M'* becomes constant at high frequencies due to the relaxation processes. Figure 13 shows that *M''* curves are asymmetric in nature. The maximum of the modulus shifted to a higher frequency indicating the increase of charge carrier. At low frequency, the value of *M'* is smaller than the maximum one because the charge carrier moves over long distances indicating the negligible contribution of electrode polarization. But at high frequency, the charge carrier moves at a short distance. The mobility of ions in amorphous glasses is in random distribution, and the effect of inter-ionic interaction gives the non-bridging oxygen.

Conclusion

Binary glass systems of the chemical composition 0.25LiO–0.75B₂O₃ and 0.25LiF–0.75B₂O₃ with low mol.% V₂O₅ were prepared using the melt-quenching method. The glassy systems were characterized by FTIR. From the results obtained it can be concluded that the vanadium ions cause small variations in the intensities of IR bands due to an increase in the glass network stability. Optical properties were measured as transmittance and absorbance. Optical band gap energies were calculated from absorbance using

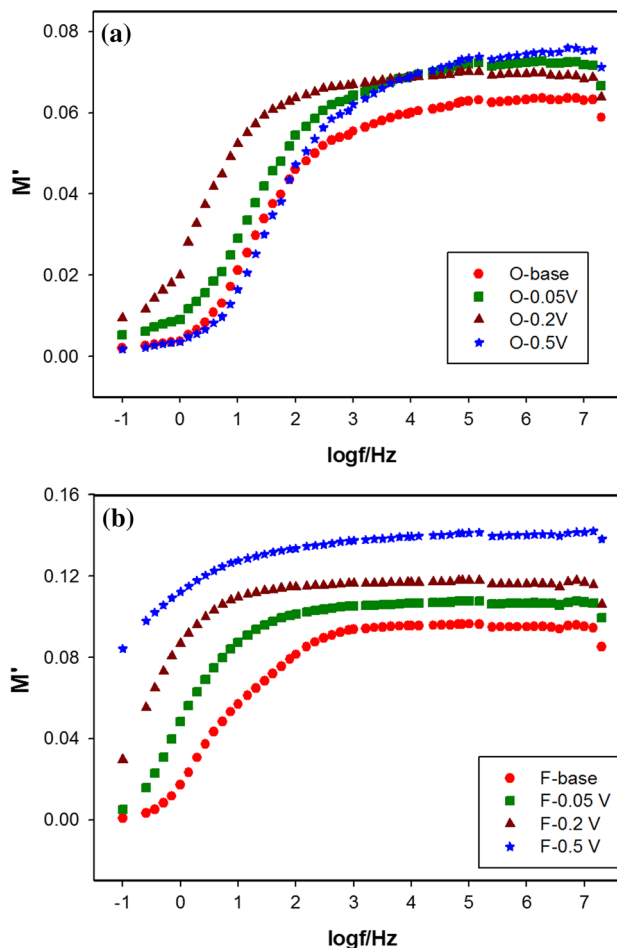


Fig. 12 Variation of real part (*M'*) of electrical modulus with frequency for of undoped and doped (a) Li₂O and (b) LiF borate glasses with vanadium oxide.

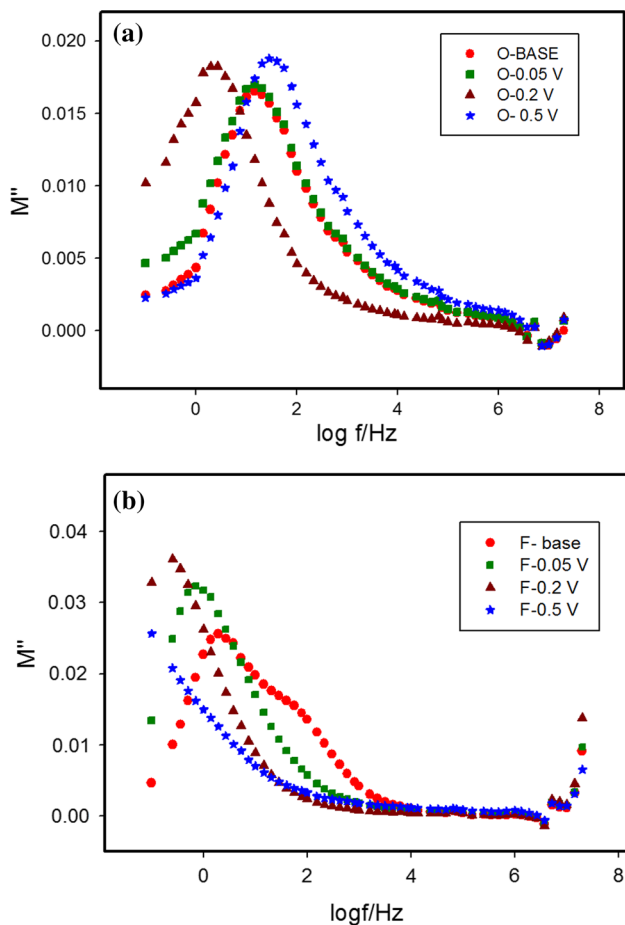


Fig. 13 Variation of imaginary part (M'') of electrical modulus with frequency for of undoped and doped (a) Li_2O and (b) LiF borate glasses with vanadium oxide.

cut-off wavelength and the Tauc equation; the small values indicate semiconducting properties. The band gap energy of oxy-borate is lower than fluoro-borate.

The ac-electrical conductivity σ_{ac} and the dielectric constant of the prepared glassy systems were studied in the range of frequency. The dielectric constant ϵ' decreased with increasing frequency and increased with the addition of vanadium. The main mechanism occurring in the base glasses is ionic conduction. In addition, in the presence of vanadium ions the conductivity increases to higher values owing to the electronic hopping in the conduction mechanism. Some vanadium ions existing in the V^{5+} valance state strengthen the structure of the glass. The ac-electrical conductivity values of the glass samples increase with frequency, indicating the semiconducting nature. This increase in oxy-lithium borate is higher than in lithium

fluoro-borate and this matches with the values of band gap energy.

This suggests that borate glasses containing V_2O_5 oxides are promising candidates to be applied in electronic devices.

Funding Open access funding provided by The Science, Technology & Innovation Funding Authority (STDF) in cooperation with The Egyptian Knowledge Bank (EKB). This research did not receive any specific grant from funding agencies in the public, commercial, or not-for-profit sectors.

Conflict of interest The authors declare no conflict of interest.

Open Access This article is licensed under a Creative Commons Attribution 4.0 International License, which permits use, sharing, adaptation, distribution and reproduction in any medium or format, as long as you give appropriate credit to the original author(s) and the source, provide a link to the Creative Commons licence, and indicate if changes were made. The images or other third party material in this article are included in the article's Creative Commons licence, unless indicated otherwise in a credit line to the material. If material is not included in the article's Creative Commons licence and your intended use is not permitted by statutory regulation or exceeds the permitted use, you will need to obtain permission directly from the copyright holder. To view a copy of this licence, visit <http://creativecommons.org/licenses/by/4.0/>.

References

1. M.Y. Hassaan, H.M. Osman, H.H. Hassan, A.S. El-Deeb, and M.A. Helal, Optical and electrical studies of borosilicate glass containing vanadium and cobalt ions for smart windows applications. *Ceram. Int.* 43, 1795 (2017).
2. S. Das, and A. Ghosh, Structure and electrical properties of vanadium boro-phosphate glasses. *J. Non-Cryst. Solids* 458, 28 (2017).
3. H. Saudi, W. Abd-Allah, and K.S. Shaaban, Investigation of gamma and neutron shielding parameters for borosilicate glasses doped europium oxide for the immobilization of radioactive waste. *J. Mater. Sci.: Mater. Electron.* 31, 6963 (2020).
4. L. Wu, A. Koryttseva, C.B. Groß, and A. Navrotsky, Thermochemical investigation of lithium borate glasses and crystals. *J. Am. Ceram. Soc.* 102, 4538 (2019).
5. A.H. Hammad, M.S. Abdel-wahab, and S. Vattamkandathil, An investigation into the morphology and crystallization process of lithium borate glass containing vanadium oxide. *J. Mark. Res.* 16, 1713 (2022).
6. M. Subhadra, S. Sulochana, and P. Kistaiah, Effect of V_2O_5 content on physical and optical properties of lithium bismuth borate glasses. *Mater. Today Proc.* 5, 26417 (2018).
7. D. Ehrhart, Phosphate and fluoride phosphate optical glasses—properties, structure and applications. *Phys. Chem. Glasses-Eur. J. Glass Sci. Technol. Part B* 56, 217 (2015).
8. C.E. Smith, and R.K. Brow, The properties and structure of zinc magnesium phosphate glasses. *J. Non-Cryst. Solids* 390, 51 (2014).
9. A. Abdelghany, and A.H. Hammad, Impact of vanadium ions in barium borate glass. *Spectrochim. Acta Part A Mol. Biomol. Spectrosc.* 137, 39 (2015).
10. F.H. ElBatal, A.M. Abdelghany, F.M.E. ElDin, and H.A. ElBatal, Vanadium structural role in binary fluoride borate glasses and

- effects of gamma irradiation. *Radiat. Phys. Chem.* 170, 108659 (2020).
11. M. Kubliha, M.T. Soltani, V. Trnovcová, M. Legouera, V. Labaš, P. Kostka, D. Le Coq, and M. Hamzaoui, Electrical, dielectric, and optical properties of $\text{Sb}_2\text{O}_3\text{-Li}_2\text{O-MoO}_3$ glasses. *J. Non-Cryst. Solids* 428, 42 (2015).
 12. X. Zhao, J. Yu, H. Cui, and T. Wang, Preparation of direct Z-scheme $\text{Bi}_2\text{Sn}_2\text{O}_7/g\text{-C}_3\text{N}_4$ composite with enhanced photocatalytic performance. *J. Photochem. Photobiol. A* 335, 130 (2017).
 13. S.Y. Marzouk, A.H. Hammad, H.M. Elsaghier, W. Abbas, and N.A. Zidan, The correlation between the structural, optical, and electrical properties in mixed alkali fluoroborate glasses containing vanadium ions. *J. Non-Cryst. Solids* 476, 30 (2017).
 14. F.M. Ezz-Eldin, N.A. Elalaily, H.A. El-Batal, and N.A. Ghoneim, Formation and bleaching of induced colour centres in gamma-irradiated vanadium-containing alkali-borate glasses. *Radiat. Phys. Chem.* 48, 659 (1996).
 15. A.M. Abdelghany, and H.A. ElBatal, Optical and μ -FTIR mapping: a new approach for structural evaluation of V_2O_5 -lithium fluoroborate glasses. *Mater. Des.* 89, 568 (2016).
 16. M.N. Khan, and E.E. Khawaja, The electrical and optical properties of glasses of the $\text{Li}_2\text{O-GeO}_2$ and $\text{Na}_2\text{O-GeO}_2$ systems. *phys. status solidi (a)* 74, 273 (1982).
 17. S.K. Deshpande, V.K. Shrikhande, M.S. Jogad, P.S. Goyal, and G.P. Kothiyal, Conductivity studies of lithium zinc silicate glasses with varying lithium contents. *Bull. Mater. Sci.* 30, 497 (2007).
 18. D.D. Ramteke, H.C. Swart, and R.S. Gedam, Electrochemical response of Nd^{3+} ions containing lithium borate glasses. *J. Rare Earths* 35, 480 (2017).
 19. D.P. Almond, G.K. Duncan, and A.R. West, The determination of hopping rates and carrier concentrations in ionic conductors by a new analysis of ac conductivity. *Solid State Ionics* 8, 159 (1983).
 20. M. Farouk, H.M. Mokhtar, Z.M. AbdEl-Fattah, and A. Samir, Vanadyl doped Li-zinc borate glasses: optical and ESR study. *J. Non-Cryst. Solids* 568, 120964 (2021).
 21. S. Salem, N.M. Deraz, and H.A. Saleh, Fabrication and characterization of chemically deposited copper-manganese sulfide thin films. *Appl. Phys. A* 126, 1 (2020).
 22. A.K. Jonscher, *Dielectric Relaxation in Solids*, Chelsea (London: Dielectrics Pub, 1983).
 23. A.M. Abdel-karim, A. Salama, and M.L. Hassan, High dielectric flexible thin films based on cellulose nanofibers and zinc sulfide nanoparticles. *Mater. Sci. Eng. B* 276, 115538 (2022).
 24. A.M. Abdel-Karim, A.H. Salama, F.A. El-Samahy, M. El-Sedik, and F.H. Osman, Some dielectric properties of novel nano-s-triazine derivatives. *J. Phys. Org. Chem.* 30, e3703 (2017).
 25. H. Doweidar, K. El-Egili, and A. Altawaf, Structural units and properties of $\text{BaF}_2\text{-PbF}_2\text{-B}_2\text{O}_3$ glasses. *J. Non-Cryst. Solids* 464, 73 (2017).
 26. H. Doweidar, K. El-Egili, R. Ramadan, and E. Khalil, Structural studies and properties of $\text{CdF}_2\text{-B}_2\text{O}_3$ glasses. *J. Non-Cryst. Solids* 481, 494 (2018).
 27. T.F. Baumann, M.A. Worsley, T.Y.-J. Han, and J.H. Satcher Jr., High surface area carbon aerogel monoliths with hierarchical porosity. *J. Non-Cryst. Solids* 354, 3513 (2008).
 28. E.I. Kamitsos, and M.A. Karakassides, A spectroscopic study of fluoride containing sodium borate glasses. *Solid State Ionics* 28, 783 (1988).
 29. D. Möncke, Photo-ionization of 3d-ions in fluoride-phosphate glasses. *Int. J. Appl. Glass Sci.* 6, 249 (2015).
 30. N. Ohtori, K. Takase, I. Akiyama, Y. Suzuki, K. Handa, I. Sakai, Y. Iwade, T. Fukunaga, and N. Umesaki, Short-range structure of alkaline-earth borate glasses by pulsed neutron diffraction and molecular dynamics simulation. *J. Non-Cryst. Solids* 293, 136 (2001).
 31. A. Bhogi, and P. Kistaiah, Alkaline earth lithium borate glasses doped with Fe (III) ions—an EPR and optical absorption study. *Mater. Today Proc.* 5, 26199 (2018).
 32. E.I. Kamitsos, Infrared studies of borate glasses. *Phys. Chem. Glasses* 44, 79–87 (2003).
 33. A.M. Abdelghanya, H.A. ElBatalb, and R.M. Ramadanc, Structural role of Li_2O or LiFon spectral properties of cobalt doped borate glasses. *J. King Saud Univ. Sci.* 29, 510–516 (2016).
 34. R.V. Barde, and S.A. Waghuley, Study of AC electrical properties of $\text{V}_2\text{O}_5\text{-P}_2\text{O}_5\text{-B}_2\text{O}_3\text{-Dy}_2\text{O}_3$ glasses. *Ceram. Int.* 39, 6303 (2013).
 35. R.M. Ramadan, A.H. Hammad, and A.R. Wassel, Impact of copper oxide on the structural, optical, and dielectric properties of sodium borophosphate glass. *J. Non-Cryst. Solids* 568, 120961 (2021).
 36. A.H. Hammad, and A.M. Abdelghany, Optical and structural investigations of zinc phosphate glasses containing vanadium ions. *J. Non-Cryst. Solids* 433, 14 (2016).
 37. S. Singh, and K. Singh, Nanocrystalline glass ceramics: structural, physical and optical properties. *J. Mol. Struct.* 1081, 211 (2015).
 38. A. Koleżyński, FP-LAPW study of anhydrous cadmium and silver oxalates: electronic structure and electron density topology. *Physica B* 405, 3650 (2010).
 39. F.H. ElBatal, H.A. ElBatal, and A.H. Hammad, The role of V_2O_5 on the structural and optical properties of $\text{MgO-ZnO-CdO-P}_2\text{O}_5$ glasses and the impact of gamma irradiation. *SILICON* 10, 831 (2018).
 40. A.A. Ali, and M.H. Shaaban, Electrical properties and scaling behaviour of Sm^{3+} doped CaF_2 -bismuth borate glasses. *Bull. Mater. Sci.* 34, 491 (2011).
 41. R. Murugaraj, G. Govindaraj, and D. George, AC conductivity and its scaling behavior in lithium and sodium bismuthate glasses. *Mater. Lett.* 57, 1656 (2003).
 42. V. Kundu, R. Dhiman, A. Maan, D. Goyal, and S. Arora, Characterization and electrical conductivity of Vanadium doped strontium bismuth borate glasses. *J. Optoelectron. Adv. Mater.* 12, 2373 (2010).
 43. A.G. Souza Filho, J. Mendes Filho, F.E.A. Melo, M.C.C. Custodio, R. Lebullenger, and A.C. Hernandez, Optical properties of Sm^{3+} doped lead fluoroborate glasses. *J. Phys. Chem. Solids* 61, 1535 (2000).
 44. S. Khasa, M. Dahiya, A. Agarwal, Effect of alkali addition on DC conductivity & thermal properties of vanadium-bismo-borate glasses, in *AIP Conference Proceedings* (American Institute of Physics, 2014), p. 796.
 45. P. Bhavani, V. Nagalakshmi, A. Iqbal, and K. Emmanuel, Structural study of $\text{PbO-PbF}_2\text{-B}_2\text{O}_3$ glass system doped with V_2O_5 through spectroscopic and magnetic properties. *Chem. J.* 3, 75 (2013).
 46. G.B. Devidas, T. Sankarappa, M.P. Kumar, and S. Kumar, AC conductivity in rare earth ions doped vanadophosphate glasses. *J. Mater. Sci.* 43, 4856 (2008).
 47. D.L. Sidebottom, Influence of glass structure on the ac conductivity of alkali phosphate glasses. *J. Phys.: Condens. Matter* 15, S1585 (2003).
 48. P. Bergo, W.M. Pontuschka, J.M. Prison, C.C. Motta, and J.R. Martinelli, Dielectric properties of barium phosphate glasses doped with transition metal oxides. *J. Non-cryst. Solids* 348, 84 (2004).
 49. A. Yadav, M.S. Dahiya, P. Narwal, A. Hooda, A. Agarwal, and S. Khasa, Electrical characterization of lithium bismuth borate glasses containing cobalt/vanadium ions. *Solid State Ionics* 312, 21 (2017).
 50. N. Krins, A. Rulmont, J. Grandjean, B. Gilbert, L. Lepot, R. Cloots, and B. Vertruyen, Structural and electrical properties of tellurovanadate glasses containing Li_2O . *Solid State Ionics* 177, 3147 (2006).

Publisher's Note Springer Nature remains neutral with regard to jurisdictional claims in published maps and institutional affiliations.

Authors and Affiliations

Amal M. Abdel-karim¹  · A. M. Fayad² · I. M. El-kashef³ · Hisham A. Saleh⁴

✉ Amal M. Abdel-karim
amalabelkarim720@gmail.com; am.abdelkarim@nrc.sci.eg

¹ Physical Chemistry Department, National Research Centre,
33 El Bohouth St., Dokki, P.O. 12622, Giza, Egypt

² Glass Department, National Research Centre, 33 El Bohouth
St., Dokki, P.O.12622, Giza, Egypt

³ Physics Department, Faculty of Science, Arish University,
Arish, Egypt

⁴ Electron Microscope and Thin Films Department, National
Research Centre, 33 El Bohouth St., Dokki, P.O.12622, Giza,
Egypt